Conference Paper, Published Version

Schoneboom, Thomas; Aberle, Jochen; Dittrich, Andreas

Hydraulic resistance of vegetated flows: Contribution of bed shear stress and vegetative drag to total hydraulic resistance

River Flow 2010 - Dittrich, Koll, Aberle & Geisenhainer (eds) - © 2010 Bundesanstalt für Wasserbau ISBN 978-3-939230-00-7

Hydraulic resistance of vegetated flows: Contribution of bed shear stress and vegetative drag to total hydraulic resistance

T. Schoneboom, J. Aberle & A. Dittrich
Leichtweiß-Institute for Hydraulic Engineering and Water Resources, Technische Universität Braunschweig, Braunschweig, Germany

ABSTRACT: Hydraulic resistance of floodplain flows depends on both drag forces exerted by vegetation elements and bed friction. Until today, the contribution of bed shear stress to total hydraulic resistance has often been neglected in hydraulic flume investigations. This has been justified with the dominance of form drag over surface friction for densely vegetated flows. However, in riparian forests where shrubs and bushes are predominant, vegetation density can be relatively low. Therefore, neglecting bed shear stress contribution can result in a significant underestimation of total flow resistance. The objective of this paper is to investigate the contribution of bed shear stress to the overall flow resistance for vegetated flows. Drag forces acting on up to 10 flexible vegetation elements were measured directly and simultaneously with specifically designed drag force measurement sensors in laboratory experiments. The measurements were carried out for three different vegetation densities, two vegetation patterns, mean flow velocities ranging from 0.1 to 0.7 m/s, and just submerged flow conditions. The hydraulic and drag force data are used to estimate bed shear stress and to assess its contribution to total hydraulic resistance dependent on vegetation density, vegetation pattern and hydraulic conditions. Existing relationships for the hydraulic resistance of vegetated flows are tested and the significance of plant specific parameters such as streamlining is highlighted.

Keywords: Vegetation, Flow resistance, Bed shear stress

1 INTRODUCTION

The ecosystems of riparian zones have high levels of biodiversity and the growing awareness of the ecological importance of these zones has resulted in the objective to maintain the functionality of channel and floodplain ecosystems (e.g. Horn & Richards, 2007). Riparian vegetation is an integral part of these ecosystems covering a wide range of conditions from highly flexible low grass to dense bushes to trees with rigid stems. However, vegetation increases flow resistance, changes backwater profiles, and modifies sediment transport and deposition (Yen, 2002). Hence, vegetation also plays a key role for flood risk assessment and sediment transport studies. Thus, it is indispensable to develop sustainable river management strategies which are in accordance with both flood plain management and ecology. The key to developing such strategies is the identification and assessment of physical processes dominating the complex interaction between water flow and vegetation.

The hydraulic resistance of vegetated channels depends on many factors including vegetation density, volumetric and areal vegetation porosities, seasonality, foliage, plant morphology, patchiness, age, plant mechanical properties, and bed surface friction. In traditional approaches vegetation has been typically reduced to boundary roughness by combining all sources of flow resistance, including vegetation, into a single bulk roughness coefficient. Such bulk coefficients have been used widely in the analysis of practical engineering problems and are typically selected with the help of reference publications (e.g., Chow, 1959; Hicks & Mason, 1999). However, bulk approaches are appropriate for one-dimensional considerations only and a detailed investigation of the influence of the vegetation on flow resistance using this approach is not possible (e.g., James et al. 2004, Wilson et al. 2006).

Based on the superposition principle (e.g., Yen, 2002) it is possible to distinguish between the contribution of surface friction and form drag to total flow resistance. Considering steady uniform

flow in a control volume with unit width and equating the driving force (downslope weight component of the water in the volume) with the resisting force of the bed and the vegetation elements yields (e.g., Petryk & Bosmajian, 1975):

$$\rho g h S = \tau_0 ' + \frac{\langle F_D \rangle}{a_x a_y} \quad (1)$$

where ρ = water density, g = gravitational acceleration, h = flow depth, S = slope, $\langle F_D \rangle$ = spatially averaged plant drag force, τ_0' = bed shear stress, and a_x, a_y = longitudinal and transversal spacing of the vegetation elements, respectively. Note that in Eq.(1) the canopy porosity has been neglected. The vegetative drag acting on a single element is usually defined as

$$F_D = \frac{1}{2} \rho C_D A_p u_c^2 \quad (2)$$

where C_D = drag coefficient, A_p = plant projected area, and u_c = characteristic approach velocity. The use of this formulation is straightforward for simple-shaped rigid objects such as cylinders. However, for complex-shaped natural vegetation C_D and A_p are difficult to determine.

Within a canopy the application of Eq.(2) becomes even more complicated as the approach velocity is not the undisturbed one. Therefore, Armanini et al. (2005) and Kothyari et al. (2009) recommend using the cross-sectionally averaged flow velocity as characteristic velocity u_c while Stone & Shen (2002) recommend using the maximum depth averaged velocity between stems. However, the latter depends on plant arrangement and is difficult to estimate for random plant arrangements.

A further problem is associated with the estimation of the drag coefficient C_D. In many studies, C_D-values have been used which were determined in experiments with single isolated stems (or cylinders) as a function of stem Reynolds number. However, these C_D-values are not appropriate for natural flexible vegetation elements and depend on the definition of plant projected area and approach velocity (e.g., Statzner et al., 2006). Furthermore, the flow structure in a canopy differs substantially from the flow structure around a single isolated element as wake flow and sheltering effects dominate the flow pattern.

Methods for the calculation of the drag coefficient for arrays of cylinders have been developed by, e.g., Li & Shen (1973) and Lindner (1982) and recent studies of Poggi et al. (2004) and Tanino & Nepf (2008) showed that the drag coefficient C_D of rigid rods decreases in canopy flows monotonically with the local stem Reynolds number due to sheltering effects. This finding is in contrast to the classical behavior of an isolated cylinder for which the drag coefficient reaches a plateau for stem Reynolds numbers ≥ 1000. Hence it is questionable if drag coefficients estimated from studies with a single vegetation element can be applied unambiguously in canopy studies. It is also not clear how the drag coefficient can be estimated appropriately for flexible and naturally shaped vegetation elements.

From experiments with single elements it is known that flexible plants bend and adapt to the flow, resulting in a more hydrodynamic shape and a reduction of flow resistance compared to stiff vegetation elements (e.g., Vogel, 1994, Järvelä, 2004; Wilson et al., 2008). This deformation directly affects the C_D-value, plant projected area A_p, and the wake flow structure. Thus, within a canopy, the vegetation elements may bend and deform slightly different and therefore one could expect slightly varying drag forces. This indicates the need for specifically designed experiments in which drag forces exerted by vegetation elements in the canopy are measured directly so that the spatial distribution of drag forces can be investigated. Eq.(1) further shows that such measurements are useful to determine bed shear stress in canopy flows (see also Aberle et al., 2010). Until today, the contribution of bed shear stress to total hydraulic resistance has often been neglected in hydraulic flume investigations. This has been justified with the dominance of form drag over surface friction for densely vegetated flows. However, in riparian forests where shrubs and bushes are predominant, vegetation density can be relatively low.

The main objective of this paper is to investigate the spatial variability of drag forces within a canopy composed of flexible elements. Based on preliminary results from specifically designed experiments, the spatial drag force variability will be discussed with regard to the canopy pattern. The data will also be used to assess bed shear stress contribution to overall resistance and to test approaches found in the literature for estimating flow resistance within canopies.

2 EXPERIMENTAL SETUP

Experiments were carried out in a 32 m long, 0.6 m wide and 0.4 m deep tilting flume in the laboratory of the Leichtweiß-Institute for Hydraulic Engineering and Water Resources, Technische Universität Braunschweig, Germany. In the experiments, the discharge Q was controlled by a valve and measured by an inductive flow meter. Water depth in the flume was adjusted by a tailgate located in a distance of 25 m to the flume inlet. Ten

piezometers installed along the flume allowed for water level measurements. These measurements were used to calculate water surface slope from linear regression and water depth h. The latter was obtained by subtracting the local flume bottom height from the piezometer readings as the flume tilted around its downstream end. The bed roughness consisted of a rubber mat with 3 mm high pyramidal shaped roughness elements.

In order to ensure fully developed canopy flow conditions, the canopy was constructed with a total length of 18.5 m starting at a distance of 6 m from the flume inlet. The canopy consisted, depending on the investigated plant pattern, of up to 450 identical artificial poplars. The 23 cm high artificial plants (see Figure 1), described in detail in Schoneboom & Aberle (2009), are composed of a 3 mm thick coated wire stem, a blossom, and four branches with three leaves each. The leaves are made of fully flexible dyed textile and the single sided leaf area varies between 14.32 to 57.6 cm^2 with a total cumulative leaf area of 373.57 cm^2. It is worth mentioning that the results described in Schoneboom et al. (2008) indicate that the flexural rigidity of the artificial poplar is similar to its 'natural' counterpart. The artificial plants were used to ensure that the plant characteristics do not change during the experiments.

The experiments were carried out with both in-line (L) and staggered (S) canopy arrangements and three different vegetation densities of 11.1, 25, and 44.4 plants/m² (spacing between plants a_x/a_y = 0.3/0.3 m, 0.2/0.2 m, and 0.15/0.15 m, respectively). Figure 2 provides an overview of the investigated vegetation patterns in the 1.5 m long test section which is located at a distance of 15.1 m to the flume inlet. In case of the densest vegetation pattern, the canopy length was reduced to a total length of 10 m starting at a distance of 10 m from the flume inlet due to the limited number of available vegetation elements. For the staggered pattern, some plants had to be placed close to the flume wall (see Figure 2). Thus, to ensure a constant plant density and a homogeneous leaf mass distribution six of the twelve leaves were removed from these plants. In addition, the plant blossom was removed from every second 'half-plant'. The additional stem in every other row affects the overall flow resistance only marginally due to the low stem diameter of 3 mm (see also Schoneboom & Aberle, 2009).

Figure 1: Setup of DFS test section and artificial poplars under flow action.

Drag forces exerted on the vegetation elements were measured with up to 10 drag force sensors (DFS) described in Schoneboom et al. (2008). The DFS were mounted in a box below the flume bottom in the test section (Figure 1). This setup ensured that the DFS did not disturb the flow and that they could be easily rearranged to match the corresponding plant patterns. The vegetation elements attached to the DFS are highlighted in Figure 2 for each setup (light gray elements).

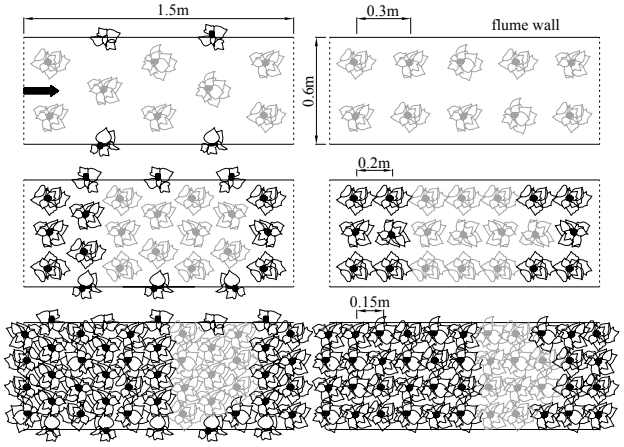

Figure 2. Vegetation setup in the measurement section (top view). Left side staggered; Right side in-line. Lateral and horizontal spacing in top-down direction 30, 20, 15 cm. Vegetation elements highlighted in grey were attached to DFS.

In contrast to the DFS setup described in Schoneboom et al. (2008), the sampling rate was reduced to 200 Hz in the present experiments. For the measurements, the DFS were synchronised and drag forces were recorded for a sampling interval of 60 s. Each measurement was repeated two times. These repeating experiments showed a high degree of reproducibility. Furthermore, a preliminary time series analysis showed that the mean value of the drag forces became, in general, stable after a sampling time of 30 s (not shown here) indicating that the sampling time of 60 sec was sufficient.

All experiments were carried out with steady uniform and just submerged flow conditions. In order to achieve these flow conditions, discharge, flume slope, and water depth were adjusted so that the deflected plants were just submerged (see Figure 1) and that the average water surface slope was identical to bed slope in the test section. The hydraulic boundary conditions are summarised in Table 1 (see end of paper) showing that 5 to 7 different flow conditions were investigated for each plant arrangement. Mean flow velocities, calculated by the continuity equation (neglecting vegetation volume) varied between u_m = 0.11 - 0.78 m/s and the water depth varied between h = 0.25 m -0.20 m. It is worth mentioning that the flow depth exceeds the blossom of the plant at the top of the element by approximately 2 cm because a part of the upper leaves were bent towards and penetrated through the water surface. As a consequence, the water depth was increased to ensure that the top parts of the plans were just submerged.

3 RESULTS & DISCUSSION

In the following we present data that enables the investigation of the spatial variability of the drag forces and the performance of existing approaches for the determination of flow resistance in canopies.

3.1 *Drag forces*

Figure 3 shows the time averaged drag forces measured for the staggered (full symbols) and inline (open symbols) setup with the lowest density (30 x 30 cm) for various mean flow velocities. The figure reveals a large variability of the measured drag forces for both arrangements. For selected plants, the relationship between F_D and u_m is shown in Figure 4 for experimental series 30S (for visual clarity only the drag forces measured by DFS01 – DFS05 are shown). Figure 4 shows that the individual relationships between F_D and u_m were approximately linear although some scatter was observed. The gradient of the straight lines varied between the elements and this variation was associated with plant deformation and sheltering effects. In fact, for the flexible elements used in this study the maximum variation of the drag force within the canopy corresponded to more than 50%. Visual observations showed that the vegetation elements did behave and deform differently although the individual elements were identical and great care was given to plant arrangement during the experimental setup to ensure that all canopy elements were aligned similarly.

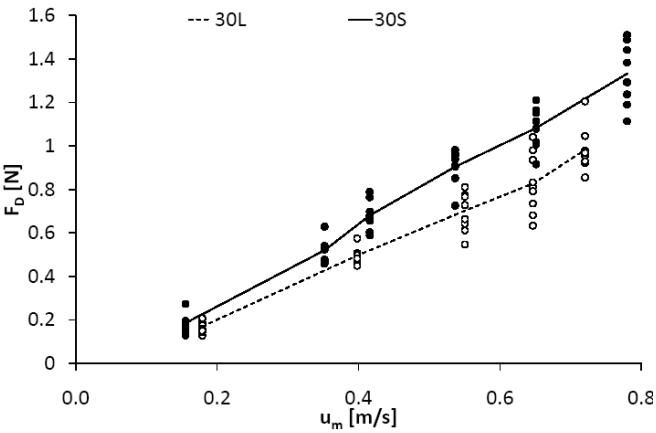

Figure 3: Spatial variability of drag forces exemplarily shown for setups 30S (full symbols) and 30L (open symbols). Each circle indicates a DFS element; lines indicate spatially averaged drag forces.

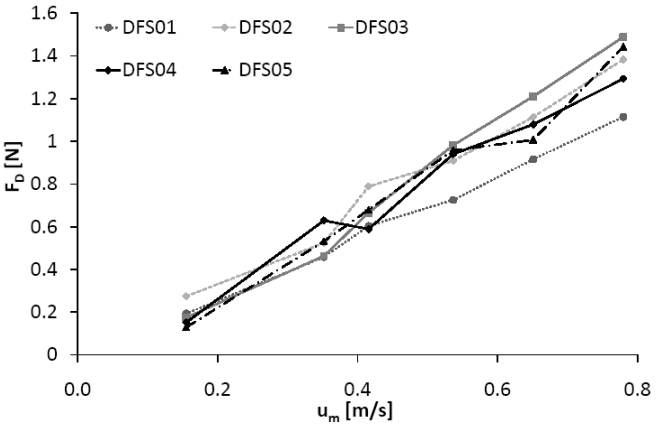

Figure 4 Drag force variability dependent on DFS

Independent of the plant arrangement it was found that the coefficient of variation (or normalized random error; defined as the standard deviation of the drag force measurements divided by the spatially averaged drag force; Bendat & Piersol, 2000) decreased with increasing flow velocity. This means that the drag force variability was larger for low flow velocities than for higher ones.

The observed spatial drag force variability indicated that it is difficult to estimate the spatially averaged drag force considering the drag force exerted on only a single element. Inasmuch this result applies to rigid vegetation elements (cylinders) will be investigated in further experiments which are currently carried out.

Despite the observed spatial variability of drag forces, the spatially averaged drag force $\langle F_D \rangle$ followed a linear relationship with mean flow velocity (solid and broken lines in Figure 3). The linear relationship was also confirmed by the results of our further measurements shown in Figure 5. A linear relationship between F_D and u_m has also been reported in studies carried out with isolated flexible elements by (e.g., Fathi-Maghadam & Kouwen, 1997, Oplatka, 1998, Armanini et al., 2005, Wilson et al., 2008). Measurements with an

isolated artificial poplar are also shown in Figure 5 and are in agreement with these findings.

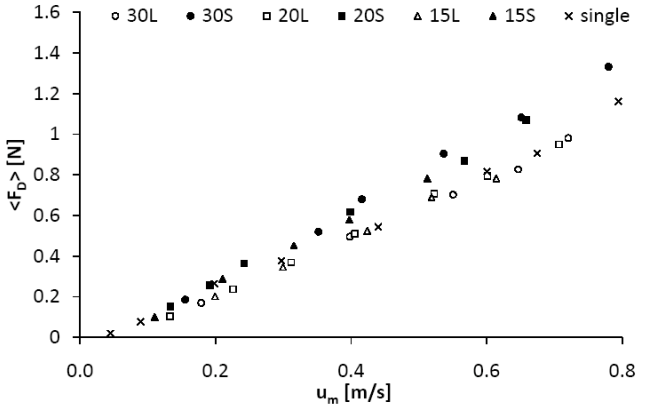

Figure 5 Spatially averaged drag forces as a function of mean velocity.

The linear relationship between F_D and u_m is generally associated with plant flexibility and deformation. In this context it is worth mentioning that the linear extrapolation of the F_D - u_m relationship towards the origin would result in negative drag forces for low velocities. This is a strong indicator that the linear relationship is only valid for larger flow velocities. This was also observed by Oplatka (1998) reporting that for very low flow velocities the F_D - u_m relationship of flexible single vegetation elements follows a squared relationship (i.e., $F_D \sim u_m^2$). In this case, the flow force is too low to deform the plants and hence the plants act as rigid bodies. The influence of plant deformation mechanisms on the F_D - u_m relationship has also been highlighted in Schoneboom & Aberle (2009).

Our data further suggests that the drag forces were consistently larger for the staggered than for the in-line pattern (Figure 5). It is also interesting to note that the F_D - u_m relationships collapsed on single lines for the staggered and in-line setup, respectively. The observed difference in drag forces indicates the importance of the flow structure within canopies (e.g., Li & Shen, 1973) affecting the approach velocity of individual plants, plant deformation (i.e., plant projected area) and as a consequence the C_D-values. In fact, our results indicated that drag force within a staggered pattern was, for comparable mean velocities, consistently 1.23 times larger compared to an in-line pattern. It is interesting to note that the F_D - u_m relationship for an isolated artificial poplar coincided with the F_D - u_m relationship of the in-line arrangement (Figure 5). The reason for this is not yet clear and this issue will be further investigated by analyzing the flow field which has been measured using Acoustic-Doppler Velocimetry (ADV). This analysis will be enhanced by considering the drag coefficients C_D which will be estimated using information on plant projected area as A_p was recorded during the experiments for each vegetation element using a submersible camera.

3.2 *Bed shear stress*

Figure 6 shows the bed shear stress τ_0', calculated using equation (1), as a function of the total stress ρghS. The figure shows that the bed shear stress increased with increasing total stress for both vegetation patterns and that the absolute value of bed shear stress depended on the vegetation spacing. For comparable total stresses, bed shear stress was, in general, largest for the lowest density and lowest for the densest canopy. Moreover, bed shear stress was larger for the in-line setup than for the staggered pattern for comparable densities. This follows also from Figure 5 where it was shown that $<F_D>$ was larger for the staggered than for the in-line setup.

However, the data shown in Figure 6 did not follow a systemic pattern and some scatter was present which we associate with the flow pattern and plant morphology. In this context it is worth mentioning that the plant shape allowed the formation of a sub-canopy flow as the leaf density close to the bed was relatively low (see Figure 1). Hence, the near bed flow velocity may resemble a jet flow regime and may be larger than the depth averaged flow velocity resulting in larger bed shear stress (e.g., Bölscher et al., 2005). This issue will also be investigated in our further analyses.

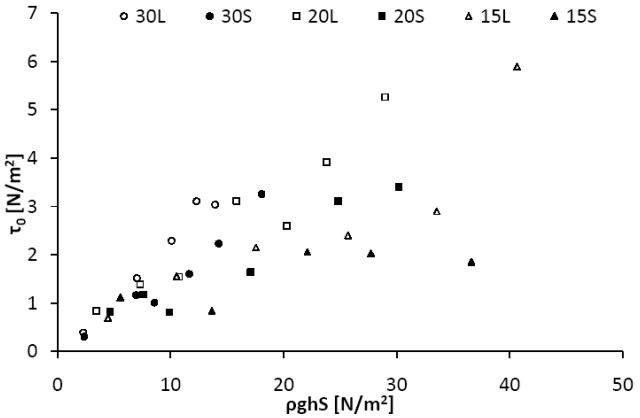

Figure 6 Bed shear stress as a function of total stress.

A closer analysis of the bed shear stress revealed that the minimum and maximum contribution of bed shear stress to total stress corresponded to 5% and 25%, respectively. The relatively large contribution of the bed shear stress to the total stress suggests that bed friction should not be neglected when investigating vegetated flows. A similar conclusion has been drawn by Righetti (2008) who found that the plant drag per unit bed surface is of the same order of magnitude as the shear resistance at the bed.

3.3 *Flow resistance*

It is common practice to express flow resistance in terms of the Darcy-Weisbach friction factor f. For vegetated flows there is the need to distinguish between surface friction and form drag using the superposition principle $f = f' + f''$ (e.g., Yen, 2002). The friction factor representing form drag f'' is defined as

$$\frac{f''}{8} = \frac{\langle F_D \rangle}{\rho u_m^2 a_x a_y} \tag{4}$$

and the friction factor representing bed friction f' can be calculated using the information on bed shear stress τ_0' according to

$$f' = \frac{8\tau_0'}{\rho u_m^2} \tag{5}$$

Existing approaches for the determination of the total flow resistance are based on the assumption that bed friction can be estimated using standard flow resistance formulae such as the Chézy-equation (e.g., Baptist et al. 2007), the log-law (e.g., DVWK 1991; Mertens 2006) or the Strickler relation (e.g., Huthoff, 2007). Using our bed shear stress estimates it is possible to test the performance of these approaches. In the following, we focus on the log-law and the Strickler relation which are defined as:

$$\sqrt{\frac{8}{f'}} = \frac{1}{\kappa} ln \frac{h}{k} + 6.27 \tag{6}$$

and

$$\sqrt{\frac{8}{f'}} = 16\sqrt{2}\left(\frac{h}{k}\right)^{\frac{1}{6}} \tag{7}$$

respectively. In these equations, κ defines the Karman constant (κ = 0.4) and k the geometric roughness height (k = 0.003 m).

Figure 7 shows the measured and calculated f'-values (using equations 6 and 7) as a function of the relative submergence h/k. The figure shows that both the Strickler formulation (eq. 7) and the log-law (equation 6) underestimate f'. At a first glance, this difference may be surprising. However, the overall resistance causing the water level h is composed of form drag and surface friction. Resistance laws such as the log-law are based on the assumption of 2D-flow conditions with surface friction as predominant source of energy loss and the existence of a logarithmic velocity profile. Such flow conditions do not prevail in vegetated flows where form drag plays an important role. For example, considering a 2D-flow where surface roughness is the only source of friction the application of Eq. (6) yields, for a given water depth, a certain discharge. If additional form roughness is present the discharge is reduced for the same water depth. Thus, as the bed roughness is not the only source of energy loss, equation (6) will not give the correct friction factor. In fact, our results showed that the effect of bed friction is generally underestimated using Eqns. (6) and (7).

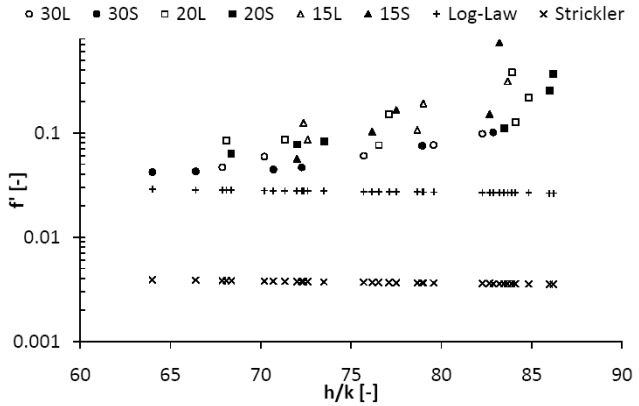

Figure 7 Observed and calculated surface friction as a function of relative submergence.

Furthermore, our results indicated that surface friction increased with increasing relative submergence. On the other hand, according to equations (6) and (7), the friction factor f' decreases with increasing water depth for 2D-flow conditions. This somehow unexpected result shows the need for further investigations focusing on the complex interaction between near bed flow, surface structure and form drag. In fact, it is not yet clear inasmuch plant deformation and plant morphology affects the results shown in Figure 7. In order to explore this issue further, we plan additional experiments with a rigid rod canopy.

As indicated by Eq. (4), form drag is often expressed in terms of f''.Our drag force data allowed the direct estimation of f'' while in other studies formulations for f'' have been derived neglecting bed surface friction. Besides, relationships derived for rigid rod canopies are not directly applicable to canopies composed of flexible elements. In the literature, only a few approaches are found which can be used to assess the form drag friction factor f'' taking into account plant specific parameters. For example, Kouwen & Fahti-Moghadam (2000) and Järvelä (2006) reported f'' - u_m relationships that can be well described by a power law. The approach of Kouwen & Fahti-Moghadam (2000) requires information on the vegetation index which depends on the resonant frequency, mass, and length of a tree. This information is not necessarily available and complicates the application of this approach. The approach of Järvelä (2004) is relatively straightforward and can be calibrated using experimental data:

$$f'' = 4\,C_{d\chi}\,LAI\left(\frac{U_{\mathrm{m}}}{U_{\chi}}\right)^{\chi}\frac{h_{\mathrm{p}}}{h} \qquad (8)$$

with $C_{d\chi}$ = species specific drag coefficient, LAI = leaf area index, U_χ = lowest mean flow velocity used when determining χ, χ = species specific vegetation parameter, and h_p = deflected plant height.

Figure 8 shows the friction factor f " normalized with leaf area index (LAI) as a function of U/U_χ. The shape of the curves are similar to the shape of the f " - u_m relationships shown in Järvelä (2006) for natural flexible vegetation. Our data showed distinct differences between the in-line and staggered setup which are associated with the aforementioned differences in drag forces (see Figure 5). Therefore, calibrating Eq. (8) resulted in $C_{d\chi}$ = 0.40, χ = -0.875, and U_χ = 0.11 m/s for the staggered and $C_{d\chi}$ = 0.28, χ = -0.765, and U_χ = 0.13 m/s for the in-line setup, respectively. These values are in the same order of magnitude as the values reported by Järvelä (2006) for natural vegetation.

Deriving Eq. (8), Järvelä (2004) assumed that the influence of plant arrangement in case of dense vegetation is insignificant but did not provide an exact value for the density limit. Furthermore, Järvelä (2002) reported that different spacing for the same number of leafless willows with grasses did not have a significant effect on the friction factor in his experiments. Fathi-Maghadam & Kouwen (1997) stated that, for non-submerged flow, the vegetation density is always a dominant parameter regardless of tree species or foliage shape and distribution. On the other hand, Li & Shen (1973) reported larger flow resistance for rigid rod canopies for staggered than for in-line patterns. The same was found in our study with relatively sparse distributions. Thus, these somewhat contradicting results indicate that the density and pattern issue should be explored in more detail in further research.

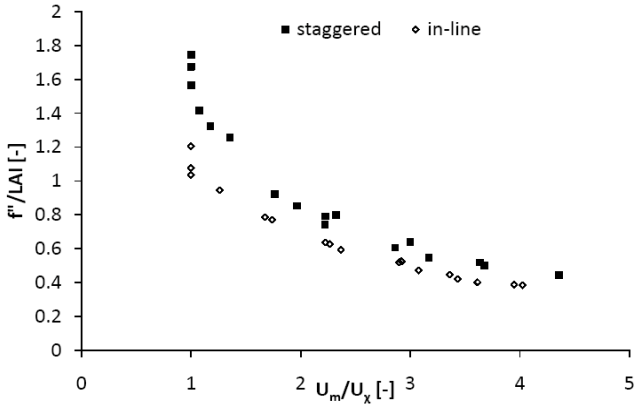

Figure 8 Friction factor f"/LAI as a function of U_m/U_X for staggered (full symbols) and in-line arrangement (open symbols).

4 SUMMARY AND CONCLUSIONS

The results presented in this paper highlight the importance of bed surface friction as well as vegetation pattern for the estimation of flow resistance in riparian zones. Using data from specifically designed experiments the spatial variability of drag forces exerted by flexible vegetation elements within a canopy was shown. In accordance with the findings for single flexible elements it was found that the spatially averaged drag force increases linearly with flow velocity and that the relationships for individual plants are also almost linear. However, the gradients for these individual relationships varied considerably indicating the complex flow structure within flexible canopies.

The results further revealed an influence of the plant pattern on both drag forces and flow resistance. It was found that flow resistance and drag forces exerted by the vegetation elements were larger for the staggered than for the in line-pattern. Similarly, it was found that bed shear stress is in general larger for the in line setup than for the staggered setup. In the experiments, bed surface friction was not negligible, as the maximum contribution of bed friction to total resistance was up to 25%. The analysis of bed friction also revealed that existing approaches underestimate bed friction.

In our future analysis we will investigate this issue in more detail using ADV-data and taking into account plant flexibility. The ADV-data will be used to describe the spatial heterogeneous flow field as well as near bed turbulence. Additional information on plant flexibility is available from photographs taken with a submersible camera. This information can be used to determine the drag coefficient C_D for single plants within the canopy and hence to develop methodologies for the estimation of vegetative drag as a function of plant specific parameters. Such data is a prerequisite for the adequate estimation of bed shear stress which, as shown in this study, is an important parameter in vegetated flows.

ACKNOWLEDGEMENTS

This research was conducted under contract AB 137/3-1 from DFG (Deutsche Forschungsgemeinschaft). The authors are grateful to U. Ecklebe for technical support and B. Herzberg and S. Niewerth for support in conducting experiments.

REFERENCES

Aberle, J., Järvelä, J., Schoneboom, T., Dittrich, A. 2010. Flow resistance of rigid and flexible emergent vegetation revisited. Proc. 1st European IAHR Congress (submitted).

Armanini, A., Righetti, M., Grisenti, P. 2005. Direct measurement of vegetation resistance in prototype scale. *J. Hydraul. Res.*, 43(5), 481–487.

Baptist, M. J., Babovic, V., Rodriguez Uthurburu, J., Keijzer, M., Uittenbogaard, R. E., Mynett, A., Verwey, A. 2007. On inducing equations for vegetation resistance. *J. Hydraul. Res.*, 45(4), 435-450.

Bendat, J. S., Piersol, A. G. (2000). Random data: analysis and measurement procedures, John Wiley & Sons, New York.

Bölscher, J., Ergenzinger, P., Obenauf, P.-J. 2005. Hydraulic, sedimentological and eco-logical problems of multifunctional riparian forest management - RIPFOR the scientific report. Heft 65, Berliner Geographische Abhandlungen.

Chow, V.T. 1959. Open-channel hydraulics. New York, McGraw-Hill.

DVWK 1991. Hydraulische Berechnung von Fließgewässern. Merkblätter zur Wasserwirtschaft, Verlag Paul Parey, Hamburg, Berlin, Merkblatt 220, in German.

Fathi-Maghadam, M., Kouwen, N. 1997. Nonrigid, nonsubmerged, vegetative roughness on floodplains. *J. Hydraul. Eng.*, 123(1), 51-57.

Hicks, D.M., Mason, P.D. 1999. Roughness characteristics of New Zealand Rivers. NIWA, Christchurch.

Horn, R., Richards, K. 2007. Flow-vegetation interaction in restored floodplain environments. Hydroecology and Ecohydrology: Past, present and future, eds. Wood, P.J., Hannah, D.M., Sadler, J.P., John Wiley & Sons, 269-294.

Huthoff, F. 2007. Modeling hydraulic resistance of floodplain vegetation. PhD thesis, University of Twente, Enschede, The Netherlands.

James, C.S., Birkhead, A.L., Jordanova, A.A., O'Sullivan, J.J. 2004. Flow resistance of emergent vegetation. *J. Hydraul. Res.*, 42(4), 390-398.

Järvelä, J. 2002. Flow resistance of flexible and stiff vegetation: a flume study with natural plants. *J. Hydrol.* 269, 44-54.

Järvelä, J. 2004. Determination of flow resistance caused by non-submerged woody vegetation. Int. J. River Basin Manag. 2(1), 61–70.

Järvelä, J. 2006. Vegetative flow resistance: characterization of woody plants for modeling applications. In: R. Graham (ed), Proc. of the World Water and Environmental Resources Congress 2006. 21-25 May 2006, Omaha, USA, papers on CD-Rom.

Kothyari, U. C., Hayashi, K., Hashimoto, H. 2009. Drag coefficient of unsubmerged rigid vegetation stems in open channel flows. *J. Hydraul. Res.*, 47(6), 691-699.

Kouwen, N., Fathi-Moghadam, M. 2000. Friction factors for coniferous trees along rivers. *J. Hydraul. Eng.*, 126(10), 732-740.

Li, R.M., Shen, H.W. 1973. Effect of tall vegetations on flow and sediment. *J. Hydr. Div.*, 99(HY6), 1085–1103.

Lindner, K. 1982. Der Strömungswiderstand von Pflanzenbeständen. Mitt. Leichtweiß-Institut für Wasserbau, Technische Universität Braunschweig, No. 75, in German.

Mertens, W. 2006. Hydraulisch-sedimentologische Berechnungen naturnah gestalteter Fließgewässer. Deutsche Vereinigung für Wasserwirtschaft, Abwasser und Abfall e.V., Hennef, in German.

Oplatka, M. 1998. Stabilität von Weidenverbauungen an Flussufern. Mitt. Versuchsanstalt für Wasserbau, Hydrologie und Glaziologie, No. 156, ETH Zürich, Switzerland, in German.

Petryk, S., Bosmajian, G. 1975. Analysis of flow through vegetation. *J. Hydraul. Div.*, 101(HY7), 871-884.

Poggi D, Porporato, A., Ridolfi, L., Alberston, J.D., Katul, G.G. 2004. The effect of vegetation density on canopy sublayer turbulence. *Boundary-Layer Meteorology*, 111, 565-587.

Righetti, M. 2008. Flow analysis in a channel with flexible vegetation using double-averaging method. *Acta Geophysica*, 56(3), 801-823.

Schoneboom, T., Aberle, J. 2009. Influence of foliage on drag force of flexible vegetation. 33rd IAHR Congress, 9-14 August 2009, Vancouver, Canada. Papers on CD-Rom.

Schoneboom, T., Aberle, J., Wilson, C.A.M.E., Dittrich, A. (2008). "Drag force measurements of vegetation elements." ICHE 2008, Nagoya, Japan, Papers on CD-ROM.

Statzner, B., Lamoroux, N., Nikora, V., Sagnes, P. 2006. The debate about drag and reconfiguration of freshwater macrophytes: comparing results obtained by three recently discussed approaches. *Freshwat. Biol.*, 51, 2173-2183.

Stone, B.M., Shen, H.T. 2002. Hydraulic resistance of flow in channels with cylindrical roughness. *J. Hydraul. Eng.*, 128(5), 500-506.

Tanino, Y., Nepf, H.M. 2008. Laboratory investigation of mean drag in a random array of rigid, emergent cylinders. *J. Hydraul. Eng.*, 134(1), 34-41.

Vogel, S. 1994. Life in moving fluids: the physical biology of flow. 2nd edition. Princeton, Princeton University Press.

Wilson, C.A.M.E., Yagci, O., Rauch, H.P., Stoesser, T. 2006. Application of the drag force approach to model the flow-interaction of natural vegetation. *Int. J. River Basin Manag.*, 4(2), 137-146.

Wilson, C.A.M.E., Hoyt, J., Schnauder, I. 2008. Impact of foliage on the drag force of vegetation in aquatic flows. *J. Hydraul. Eng.*, 134(7), 885-891.

Yen, B. C. 2002. Open Channel Flow Resistance. *J. Hydraul. Eng.*, 128(1), 20-39.

Table 1 Experimental boundary conditions

Index	spacing [m]	pattern	No. of DFS	No. of flow conditions	Slope S [%]	h [m]	Q [l/s]	u_m [m/s]
30S	0.30	staggered	8	6	0.097 - 0.924	0.249 - 0.198	23.15 – 93.3	0.155 – 0.78
30L	0.30	in-line	8-9	5	0.094 – 0.698	0.247 – 0.204	26.5 - 88	0.179 – 0.72
20S	0.20	staggered	10	6	0.183 – 1.5	0.259 – 0.205	20.7 - 81	0.13 – 0.66
20L	0.20	in-line	10	7	0.14 – 1.447	0.254 – 0.204	20 - 86.6	0.13 – 0.706
15S	0.15	staggered	8-9	5	0.227 – 1.73	0.25 – 0.216	16.5 – 66.4	0.11 – 0.512
15L	0.15	in-line	7-8	5	0.428 – 1.91	0.251 – 0.217	30 - 80	0.20 – 0.615